

## Magnetization of Solid $^3\text{He}$ through the Nuclear Ordering Temperature

T. C. Prewitt and J. M. Goodkind

*Department of Physics, University of California, San Diego, La Jolla, California 92093*

(Received 15 September 1977)

We have measured the static nuclear magnetization of solid  $^3\text{He}$  as a function of temperature and molar volume through its nuclear ordering temperature. Below 5 mK the magnetization increases with decreasing temperature more rapidly than the Curie-Weiss behavior displayed at higher temperatures. At  $T_S$  it decreases rapidly to 40% of its maximum value and becomes temperature independent at the lowest temperature we measure.  $T_S$  decreases with decreasing molar volumes.

Solid  $^3\text{He}$  is a uniquely simple system for applying and testing the various theories of magnetism. Its atomic angular momentum derives entirely from the one-half spin of its nucleus, it has a body-centered cubic lattice, and there is sufficient overlap of the atomic wave functions so that quantum exchange forces dominate the magnetic behavior. Historically its behavior has been interpreted in terms of the Heisenberg Hamiltonian

$$H_{nm} = -2J \sum_{\substack{nm \\ i < j}} \vec{I}_i \cdot \vec{I}_j - \vec{H} \cdot \sum_i \vec{\mu}_i,$$

where  $J$  is the exchange energy, the sum over  $i$  and  $j$  with  $i < j$  is taken only over nearest-neighbor (nn) spins  $I_i$  and  $I_j$ ,  $\vec{H}$  is the applied magnetic field, and  $\vec{\mu}_i$  the magnetic moment of the  $i$ th spin. A mean-field calculation on the above Hamiltonian leads to the Curie-Weiss law for the magnetization,  $M$ ,

$$M = C / (T - \theta),$$

where  $C$  is the Curie constant and  $\theta$  is equal to  $4J$ . Early measurements of  $M$  at temperatures above 5 mK could be fitted to this law with  $\theta$  negative,<sup>1</sup> indicating that the system would order antiferromagnetically if the model was applicable. More recent measurements<sup>2-5</sup> are inconsistent with this Hamiltonian so that more complicated ones which include next-nearest neighbor and three- and four-atom exchanges have been proposed and are being studied.<sup>6-9</sup> The behavior at temperatures just above and below the ordering temperature is of critical importance to understanding the nature of the ordered state. We report here the first measurement of the solid  $^3\text{He}$  magnetization in that range. The ordering observed is antiferromagneticlike in that the magnetization decreases below the critical temperature rather than increasing as in the case of a ferromagnet. However, its behavior is inconsis-

tent with that derived from the above Hamiltonian. Substantial new constraints are imposed on future theories by these results.

The apparatus for this work, shown in Fig. 1, was similar to those used previously in this laboratory.<sup>10</sup> Cooling was achieved by adiabatic demagnetization of copper nuclei. NMR measurement of the Curie susceptibility of the same nuclei provided the thermometry. Calibration of the thermometer was performed against the susceptibility of a cerium magnesium nitrate powder sample which was itself calibrated against the

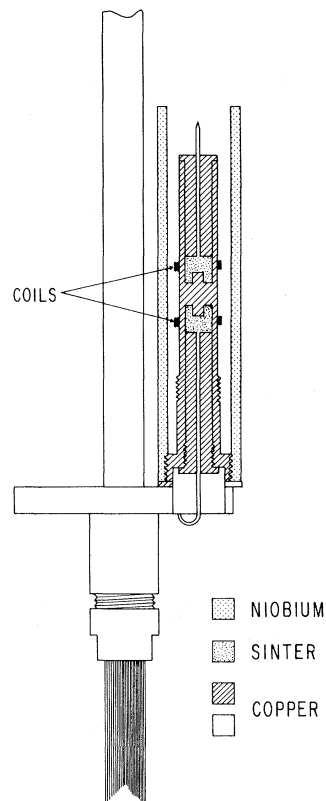


FIG. 1. Schematic drawing of sample cell.

vapor pressure of  $^4\text{He}$ . Statistical error in the calibration were estimated to be  $\pm 10\%$ .

The sample cell consisted of two identical chambers which were packed with copper powder and sintered leaving a surface area of  $1.1\text{ m}^2$  and a volume of  $0.09\text{ cm}^3$ . One of the chambers was used to hold the sample and the other was evacuated. Two identical but oppositely wound niobium coils were wrapped on the chambers and connected in series with a superconducting transformer. A point-contact superconducting magnetometer (SQUID) was coupled to the transformer and used to sense magnetic flux changes induced by the temperature dependence of the sample magnetization. The sample was in a constant magnetic field trapped by a concentric niobium cylinder.

Solid  $^3\text{He}$  samples were prepared by pressurizing liquid  $^3\text{He}$  to the desired density at  $1.5\text{ K}$ . A plug of solid  $^3\text{He}$  was then formed by cooling a section of the capillary tube leading to the sample. The sample was then cooled to  $16\text{ mK}$  over a period of  $24\text{ h}$ . The copper demagnetizations were performed from this temperature and resulted in a minimum temperature of  $0.5\text{ mK}$  for the copper. The lowest temperature at which thermal equilibrium between copper and  $^3\text{He}$  could be demonstrated was  $0.8\text{ mK}$ . The temperature dependence of the  $^3\text{He}$  magnetization as sensed by the SQUID was then recorded during the subsequent warmup under the residual heat leak. Warmup rates at the  $^3\text{He}$  transition temperature varied from  $0.3$  to  $0.6\ \mu\text{K}/\text{min}$ . The signal due to incomplete cancellation of the background magnetization was measured with liquid  $^3\text{He}$  in the cell at the pressure of the melting-curve minimum. In the temperature range measured the susceptibility of the liquid is two orders of magnitude less than that of the solid and above the superfluid transitions is temperature independent. The background signal was subtracted from the signal obtained with solid in the cell and the difference was attributed to the solid. The measurements with liquid in the cell did not reveal the drop in magnetization at the  $A$ -to- $B$  liquid transition. This may be a consequence of the small size of the pores in the sintered copper sponge.

The results for a sample with molar volume  $24.2\text{ cm}^3$  are shown in Fig. 2. Below  $5\text{ mK}$ , its inverse magnetization lies below the Curie-Weiss extrapolation with  $\theta = -2.6\text{ mK}$ . At  $1.25\text{ mK}$ , the magnetization is a factor of 2 larger than the Curie-Weiss value at that temperature. Below  $1.25\text{ mK}$  the magnetization decreases rapidly until at  $1.05\text{ mK}$  it is  $40\%$  of its peak value. From

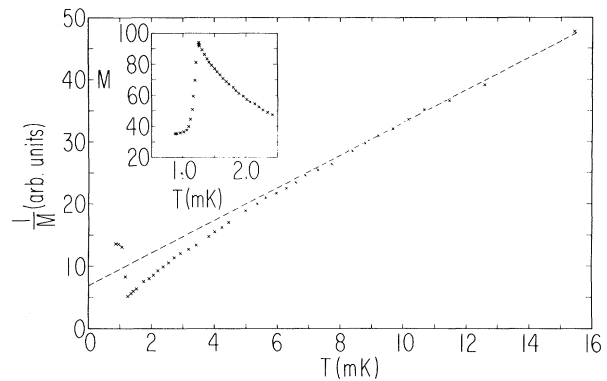


FIG. 2. Inverse magnetization of solid  $^3\text{He}$  at molar volume  $24.2\text{ cm}^3$ . Dashed line is Curie-Weiss behavior; crosses are data points. Data is a composite of two runs with the data from one shown below  $1.5\text{ mK}$  and from the other above  $1.5\text{ mK}$ . The inset shows data from one run only.

this temperature down to  $0.9\text{ mK}$  the magnetization is nearly temperature independent. The temperature measured is that of the copper coolant and not of the  $^3\text{He}$  itself. If there were an actual discontinuity in the magnetization, disequilibrium between copper and  $^3\text{He}$  would smear it out and lead to artificially high, apparent transition temperatures. We observe that the transition becomes steeper as the warmup rate decreases, so that our results are consistent with a discontinuous transition at  $T = 1.05\text{ mK}$ . The largest uncertainty in this determination is the  $\sim 10\%$  statistical uncertainty of the calibration of the NMR thermometer.

In addition to the magnetization, it was also possible to obtain a rough measurement of the  $^3\text{He}$  heat capacity by observing its effect on the warmup rate of the copper- $^3\text{He}$  system as a function of temperature. With solid in the cell, a plot of the warmup rate displayed a sharp minimum at the temperature of the magnetization maximum.

Samples with molar volumes of  $24.0$  and  $23.7\text{ cm}^3$  were also measured. Qualitatively, their behavior was found to be the same as that of the  $24.2\text{-cm}^3/\text{mole}$  sample displayed in Fig. 2, except that the temperatures of the magnetization peaks were lower by  $0.09$  and  $0.27\text{ mK}$ , respectively.

Most of the measurements were made in a field of  $500\text{ G}$ , but one sample was measured in a field approximately one-third of that. The magnetization was found to scale uniformly over the temperature range measured, within the uncertainties due to the thermal disequilibrium discussed

above.

Because of the small size of the sample chamber, a large uncertainty in the molar volumes of the samples prepared by the method described was expected. In order to test the method, a sample was prepared such that its expected molar volume would require it to consist partly of liquid and partly of solid. As a consequence of being on the melting curve, its solid would necessarily have a molar volume of 24.22 cm<sup>3</sup>/mole. Apart from a scale factor that we assume to be the proportion of the sample that was solid, the results for that sample agreed with those of a sample prepared to be entirely solid at the same molar volume. Thus, for this molar volume at least, the method was reliable.

The results presented here are consistent with those presented previously by other authors. Our measurements are in agreement with the measurements of Bernier and Delrieu<sup>11</sup> and of Bakalyar *et al.*<sup>12</sup> in the temperature range in which those authors have measured the magnetization. Our observation of a large thermal anomaly at  $T_S$  is in agreement with the results of Halperin *et al.*<sup>4</sup> The deviation from a Curie-Weiss behavior for temperatures below 5 mK may be related to the heat-capacity deviation from  $1/T^2$  measured by Dundon and Goodkind.<sup>3</sup> Finally, by applying the Maxwell relation,

$$(\partial S/\partial H)_T = (\partial M/\partial T)_H,$$

and the magnetic Clausius-Clapeyron equation,

$$dH/dT = -\Delta S/\Delta M,$$

to the data of Kummer, Mueller, and Adams,<sup>5</sup> we find their results to be consistent with the magnetization behavior that we measure.

The theoretical picture is not as clear. Roger, Delrieu, and Landesman<sup>13</sup> have found that by including in a model Hamiltonian the effects of exchange of up to four particles, they can fit the data of Bernier and Delrieu<sup>11</sup> with the values  $\theta = -3.6$  mK and  $B = -2.8$  mK<sup>2</sup> in the expression

$$\chi^{-1}(T) = N^{-1}K(2/\gamma\hbar)^2(T - \theta + B/T + \dots)$$

for the solid susceptibility. Using the value of  $\theta = 2.6$  mK, we are able to fit our data with  $B = -2.7 \pm 0.5$  mK<sup>2</sup>. However, the theory of Roger, Delrieu, and Landesman predicts only a slight decrease in  $M$  at the transition, which is in conflict with the 60% reduction that we measure. Heritier and Lederer<sup>14</sup> suggested that the excess magnetization above the Curie-Weiss value could be attributed to a vacancy effect that would be

gradually "frozen out" for temperatures below the transition leaving only the Curie-Weiss value. The magnetization we measure below the transition is, in fact, the same as would be obtained from a Curie-Weiss behavior with a Néel temperature of 2.5 mK and the usual temperature-independent behavior below that. However, this model assumes a density of vacancies of  $2.5 \times 10^{-4}$  for the melting-curve molar volume. It is expected that even if this density were correct on the melting curve, it would fall off rapidly for smaller molar volumes. Thus the qualitatively similar behavior of the samples with molar volumes 24.0 and 23.7 cm<sup>3</sup> to that of the samples near the melting curve would be difficult to explain.

In conclusion, we have presented the first measurements of the solid-<sup>3</sup>He magnetization below its ordering temperature. We demonstrate for the first time that the solid transition previously reported for samples on the melting curve persists for molar volumes off the melting curve. We find good agreement of our results with those reported by other experimentalists, but find difficulty in interpreting the results with available theories.

<sup>1</sup>W. P. Kirk, E. B. Osgood, and M. Garber, *Phys. Rev. Lett.* **23**, 833 (1969); J. R. Sites, D. D. Osheroff, R. C. Richardson, and D. M. Lee, *Phys. Rev. Lett.* **23**, 826 (1969); P. B. Pipes and W. M. Fairbank, *Phys. Rev. Lett.* **23**, 520 (1969); T. P. Bernat and H. D. Cohen, *Phys. Rev. A* **1**, 1709 (1973).

<sup>2</sup>W. P. Kirk and E. D. Adams, *Phys. Rev. Lett.* **27**, 392 (1971).

<sup>3</sup>J. M. Dundon and J. M. Goodkind, *Phys. Rev. Lett.* **32**, 1343 (1974).

<sup>4</sup>W. P. Halperin, C. N. Archie, F. B. Rasmussen, R. A. Buhrman, and R. C. Richardson, *Phys. Rev. Lett.* **32**, 927 (1974).

<sup>5</sup>R. B. Kummer, R. M. Mueller, and E. D. Adams, *J. Low Temp. Phys.* **27**, 319 (1977).

<sup>6</sup>L. I. Zane, *J. Low Temp. Phys.* **9**, 219 (1972).

<sup>7</sup>A. K. McMahan and J. W. Wilkens, *Phys. Rev. Lett.* **35**, 376 (1975).

<sup>8</sup>J. H. Heatherington and F. D. C. Willard, *Phys. Rev. Lett.* **35**, 1442 (1975).

<sup>9</sup>M. Roger, J. M. Delrieu, and A. Landesman, *Phys. Lett.* **62A**, 449 (1977).

<sup>10</sup>J. M. Dundon, D. L. Stofa, and J. M. Goodkind, *Phys. Rev. Lett.* **30**, 843 (1973).

<sup>11</sup>M. Bernier and J. M. Delrieu, *Phys. Lett.* **60A**, 156 (1977).

<sup>12</sup>D. M. Bakalyar, E. D. Adams, Y. C. Hwang, and C. V. Britton, in *Proceedings of the Quantum Crystal Conference*, Fort Collins, Colorado, 8-12 August

1977, edited by James R. Sites (to be published), Abstract 37.

<sup>13</sup>M. Roger, J. M. Delrieu, and A. Landesman, in Proceedings of the Quantum Crystal Conference, Fort

Collins, Colorado, 8-12 August 1977, edited by James R. Sites (to be published), Abstract 52.

<sup>14</sup>M. Heritier and P. Lederer, J. Phys. (Paris), Lett. **38**, 209 (1977).

## Observation of Forbidden Brillouin Scattering near an Exciton Resonance

G. Winterling, E. S. Koteles, and M. Cardona

Max-Planck-Institut für Festkörperforschung, 7 Stuttgart 80, Federal Republic of Germany

(Received 1 September 1977)

We have observed resonant Brillouin scattering by TA phonons near the  $A$  exciton of CdS in a usually forbidden backscattering configuration. This effect, attributed to electron-phonon piezoelectric coupling, is equivalent to the Fröhlich-interaction-induced forbidden LO scattering. A numerical estimate of the scattering strength of the forbidden TA scattering accounts for the intensity of the observed lines.

Fröhlich-interaction-induced resonant forbidden Raman scattering by *longitudinal* optical phonons has been extensively investigated in semiconductors.<sup>1</sup> In this Letter we show that a similar effect exists for *transverse* acoustic phonons and we present, for the first time to our knowledge, experimental evidence of resonant forbidden Brillouin scattering. The macroscopic electric field required for the Fröhlich interaction is, in this case, produced by the strain-induced longitudinal piezoelectric polarization, i.e., by the piezoelectric coupling between TA and LO modes. Surface electric field or impurity-induced forbidden scattering can be ruled out since it would not conserve the vector  $\vec{q}$  thus leading to broad structures in scattering by acoustic phonons.

Our measurements were performed in the regime of resonant polariton scattering discussed by Brenig, Zeyher, and Birman<sup>2</sup> and experimentally observed for allowed LA scattering by Ulrich and Weisbuch<sup>3</sup> in GaAs, and by Winterling and Koteles<sup>4</sup> in CdS. Our samples were vapor-grown single-crystal CdS platelets with smooth, unpolished surfaces and a thickness of  $\sim 10^{-2}$  cm. The Brillouin spectra were excited by the focused beam of a tunable narrow-band ( $\leq 0.4$  cm<sup>-1</sup>) cw dye laser (Coumarin 102) with the sample at  $T \sim 6$  K. The incident power density was of the order of 1 W/cm<sup>2</sup>. Both the incident and the backscattered light propagated with  $\vec{k}$  perpendicular to the hexagonal  $c$  axis and their electric fields were also perpendicular to  $c$ . Thus the scattering wave vector  $\vec{q}$  was perpendicular to the  $c$  axis and, consequently, the scattering phonons are

either purely longitudinal or purely transverse. The backscattered light was spectrally analyzed with a double-grating monochromator. The combined spectrometer and dye-laser width was 0.7 cm<sup>-1</sup>.

The principle of resonant polariton (back-) scattering is illustrated in Fig. 1(a). The exciton-polariton dispersion relation of CdS in the vicinity of the  $A$  exciton was obtained from the dielectric function<sup>6</sup> with the parameters given in Fig. 1. Contrary to the ordinary picture of resonant scattering which involves *virtual* excitons as intermediate states, polariton scattering takes place between two real polariton states. The allowed LA backscattering, indicated by the dashed lines in Fig. 1(a), is that reported in Ref. 4 and shown also in Fig. 2.

The corresponding backscattering by TA phonons is, for  $q \rightarrow 0$ , forbidden by symmetry. The shear strains in this case modulate only that component of the optical-frequency dipole moment which is parallel to the  $\vec{q}$  of the TA phonon and which, consequently, cannot radiate in the backward ( $\vec{q}$ ) direction. This argument applies equally to deformation-potential coupling and to coupling through the first-order electro-optic effect.

Strong resonant forbidden LO Raman scattering<sup>1</sup> has been observed in CdS. It is induced by the macroscopic longitudinal electric field of the LO phonon through the Fröhlich interaction. Since the slow TA phonon also has a *longitudinal* electric field (piezoelectric effect), as one sees from an inspection of the piezoelectric tensor, resonant forbidden TA scattering in analogy to the forbidden LO scattering should take place. We